Simulation of Soil Movement in Geotechnical Centrifuge Testing – Deep Excavations, Tunnelling, Deposit

D. König[1], O. Detert[2] and T. Schanz[1]
[1]*Institute for Foundation Engineering, Soil and Rock Mechanics, Ruhr-Universität Bochum, Bochum, Germany*
[2]*HUESKER Synthetic GmbH, Gescher, Germany*
E-mail: diethard.koenig@rub.de

ABSTRACT: Foundation engineering works are mostly related to movement of soil masses. Excavation of construction pits and of tunnels, construction of embankments and dams, all these activities impose the take of, transport and deposit of more or less huge amount of soil masses. These processes of soil movement lead to change of stress, activation of shear resistance and deformation in the remaining or underlying soil. To control such effects special works like installation of retaining structures, soil stabilisation by nailing or injection, improvement of drainage conditions or others are carried out. These measures have to be designed taking into account the interaction with the surrounding soil and the construction process. Up to now not all of the relations between the different construction elements and soil reactions are fully understood. Independent on the progress in numerical modelling physical modelling is helpful to discover and analyse such interactive reactions. For this it is necessary to simulate soil movement in physical modelling. Especially in centrifuge modelling this is a challenge. Within this paper an overview is given of different methods to simulate soil movements in the geotechnical centrifuge and three examples on projects carried out in the Bochum Geotechnical Centrifuge ZI are described more in detail. The main topics are the excavation of construction pits, the excavation of tunnels and the deposit of soil masses.

1. INTRODUCTION

Prediction of ground movements arising from foundation works or tunnelling becomes more and more important. Density of infrastructure is increasing especially in urban areas and the sensitivity of historic or sophisticated structures gain in the focus of authorities and public interest. The complex behaviour of the soil and the multiple interactions between soil, construction procedures and structures force to improve numerical methods. Up-to-date constitutive models are taking into account stress path depending soil behaviour, small strain stiffness and time depending effects. Computer capacity allows to model complex three dimensional situations including a high degree of detailing. Nevertheless it is still a challenge to decide on the correct boundary conditions, to choose an appropriate idealisation, which is still necessary, and to assess the different parameters. Due to this a calibration and validation of our models is essential, which can be realised by comparing the numerical results with field measurements. Otherwise physical modelling gives the chance to compare numerical data with physical measurements on a prototype implying all selected characteristics of the real field situation under well known boundary conditions, e.g. by centrifuge modelling. This premises sufficient techniques to display the major aspects of the field situation and to reproduce the relevant stress paths.

One important aspect considering this background is the simulation of soil excavation and soil deposit procedures also in centrifuge modelling under high acceleration levels, which has been developed since many decades. In this paper three processes are selected to give a short overview on the development of the model technique and for each process one example for a test design is described. These test designs have been developed at Ruhr-Universität Bochum and are used in the Bochum Geotechnical Centrifuge ZI, which characteristics are described by Jessberger & Güttler (1988).

2. CONSTRUCTION PITS

2.1 Methods

Different methods have been used to simulate an excavation in centrifuge modelling. Lyndon & Pearson (1984) modelled the behaviour of sheet pile walls in sand. The sheet pile model was located in the final position in the strong box and the soil has been placed around. The strong box was exposed to the selected g-level. After reading the data of the different transducers the centrifuge was stopped and an excavation step performed at 1 g. This procedure has been repeated several times. Using this method a sequence of loading and unloading procedures is applied to the soil and the structure, which do not represent field conditions.

Bolton & al. (1988) simulated the excavation of a retaining wall in overconsolidated clay by replacing the soil in the excavation zone by a rubber bag filled with a zinc chloride solution and draining the fluid after a reconsolidation period. The zinc chloride solution was mixed to the same unit weight like the clay and therefore an initial effective earth pressure coefficient of $K_0 = 1$ was applied, which may correspond to earth pressure conditions in overconsolidated clays. A fluid support has been chosen also by Toyosawa at al. (1994) (zinc chloride), Lade & al. (1981) (paraffin oil) and Schürmann & Jessberger (1994) (water), which allow to simulate smaller earth pressure coefficients, or Zheng et al.(2010).

After placing the model soil in the strong box Azevdo (1983, 1988) removed the wet sand within the zone which should be later excavated. Then a bag of fabric was placed all along the contour of the later excavation at 1g and the removed soil was filled inside the bag again. After exposing the model to higher g-level the excavation was simulated by lifting up the bag with the soil inside using an electric motor. The excavation is simulated in one step, not as a continuous procedure. A similar system has been developed by Allersma (1998) using also a fabric which is placed by loops in different layers and which allows a stepwise excavation. The influence of the reinforcement on the soil behaviour by the fabric is unknown using such techniques.

In 1994 Kimura at al. presented an in-flight excavator used in soft clay. The excavator removes the soil by scraping layer for layer (5 to 10 mm thick). This scraping technique has been modified by Loh at al. (1998) to simulate a three dimensional excavation. Such a procedure could also be performed with an on-board robot as presented by Derkx at al (1998) and Gaudin et al. (2002). A 2D servo-actuator has been developed at University of Cambridge (Haigh et al. 2010) and used for the simulation of the excavation by scraping in soft clay in front of a retaining wall, which is supported by props (Lam et al. 2010). The scraping technique does not allow a lift up of the soil which has to be excavated. Due to this the soil has to be moved throughout a barrier. The top edge of the barrier has to be on a lower level compared to the soil moved by the scraper. The barrier has to be removed step by step or has to be lowered continuously with the excavation. This can be realised by removing a segmented wall step by step or by a moving wall system. This method is up to now the most realistic way to simulate field conditions and has been chosen for a series of tests in the Bochum

Geotechnical Centrifuge ZI for studying the earth pressure distribution acting on an anchored sheet pile wall (König 2002).

2.2 Bochum in-flight excavator for deep excavations

2.2.1 Design

The model set up is shown in Figure 1. The model is built up within a strong box with internal dimensions of 630 mm in length, 360 mm in width and 700 mm in height. The soil sample is placed inside the box including the model wall (3), which could be supported by one or two anchor levels. The position of the surface of the soil inside of the strong box depends on the length of the model wall, the number and position of anchors. At each anchor level a waling supported the model wall made of a steel bar with a cross section of about 4 to 8 mm.

Two steel rods (4) with a diameter of 2 mm are screwed into the waling and are passing the back wall of the strong box (figure 2). Each of them is connected first to a load cell (a) and then to a pulley (7) which is fixed on an axle (b) mounted at the back of the box. A gear weal (c) is also fixed on this axle and could be loaded by a chain with a counterweight (5) and a water container (6) at it ends. The water container can be filled by open the valve between the container and the water reservoir (11) on top of the box. Additionally the pulley can be blocked by a break (d), which is activated by air pressure (10). In that case no more displacement of the anchors can occur.

The front wall (2) is mounted movable hanging on two chains balanced by counterweights (9). The position is controlled by an electric chain drive placed on the top of the strong box. The wall is sealed against the box by a rubber membrane. Sliding occurs during lowering of the front wall between the front wall and plastic stripes glued in a horizontal position one above the other on the rubber membrane.

On top of the strong box the excavation mechanism is placed which is designed similar to the device presented by Kimura at al. (1993, 1994). The scraper (1) could be moved back and forth as well as up and down controlled by electric motors. In front of the strong box a second box (8) is placed to collect the excavated soil.

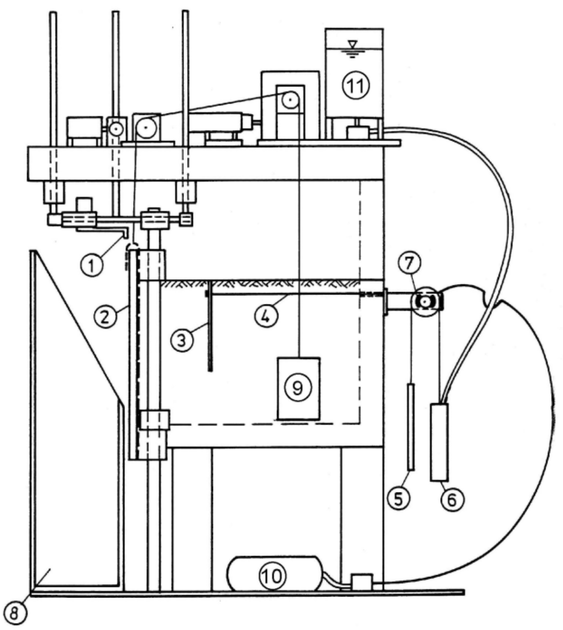

Figure 1 Model set up (explanation see text)

The tests described in this paper have been performed with a fine grained sand used by Schürmann & Jessberger (1994). After fixing the strong wall in the initial position the side walls and the back wall of the strong box have been lubricated by a fine grease and covered by a plastic folio to reduce wall friction as fare as possible. The sand is placed by pluviation with a density of 1.68 g/cm³, which is close to 100 % relative density, up to the level of the toe of the model wall. The model wall with the waling is placed by a temporary support in the final position as well as the LVDT detecting the displacements at the toe of the wall.

The pluviation of the sand continues on both sides of the wall until an anchor level is reached. Then the anchor rods are placed within small tubes to reduce friction and connected to the waling as well as to the load cells and pulleys. In that moment the anchors are slackly embedded in the sand only stressed by a small pre-load due to a little bit of water inside the water containers (Figure 1, No. 6). The LVDT's to measure the horizontal displacements at anchor level are placed at the same time. The pluviation is continued until the final soil surface is reached. Now the excavator, the chain drive for the front wall and the water reservoir for loading the anchors are mounted on the top of the box.

2.2.2 Test procedure

The tests have been performed at an acceleration level of n = 30. The excavation starts after reaching this acceleration level with a short delay. First the front wall is lowered by about 3 cm. This leads to a failure in the sand close to the top of the front wall and some sand falls into the soil collecting box. A slope remains above the top of the front wall. This area is outside the active shear zone in front of the model wall so it is assumed that there is no influence on the model wall behaviour.

Now the scraper is moved close to the model wall and is pushed for a few millimetres (model dimension) into the sand. A layer of sand is removed and is slipped over the top of the front wall. The sand falls into the soil collection box. The scraper moves up and is driven back to the model wall to repeat the procedure. In front of the model wall a small slope remains, which height depends on the amount of each excavation step and the distance between scraper and model wall during penetration of the scraper into the soil. In the reported tests the height of this slope was about 2 cm (model dimensions).

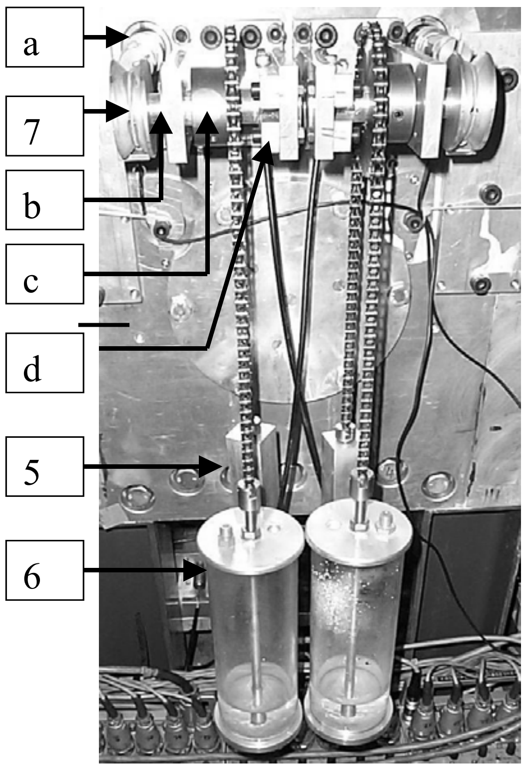

Figure 2 Fixation of anchors at the back wall of the strong box

After a series of excavation steps the front wall is lowered again. Reaching an anchor level the excavation is continued up to about 50 cm in prototype dimensions below the waling. Now the valve between the water reservoir (Figure 1, No 11) and the water container (6) is opened and the anchor, which has been loaded only by a small pre-load up to now, is loaded up to a defined force. Then the pulleys (7), which are connected with the anchors, are fixed by the breaks mentioned above. The excavation is continued up to the selected excavation level or up to the moment where large deformations of the model wall indicate failure of the soil in front of the model wall.

2.2.3 Test results

Figure 3 shows the bending moment distributions measured at different excavation depths by pairs of strain gauges placed on both sides of the model wall along a cross section in the centre of the wall. At the beginning only very small bending moments are measured. The distribution is randomly. Also with the first excavation steps the load on the wall is small. Typical positive moments are observed at anchor level after tightening of the anchors. With further excavation the moments at anchor level increased as well as the negative moments in the field. The rate of increase of bending moment at anchor level becomes smaller compared to the rate of increase of the bending moment in the field after five meters excavation. This may be due to the limited bearing capacity of the soil above the anchor, where the wall moves in direction of the soil and passive earth pressure conditions develops.

The change of the interaction between soil and sheet pile wall in the lower part of the wall is obvious. The positive moments indicate a fixation of the wall in the soil. This moments disappear with continues excavation.

Processed test data are presented in Figure 4. The measured bending moments are approximated by spline functions as explained by Schürmann & Jessberger (1994). Due to the singularity at the anchor level two splines are used, one for the upper and one for the lower part. For this procedure it is necessary to introduce different boundary conditions. Most of them are well known by the measurements, some of them have to be estimated from the overall data. For example the exact bending moment at anchor level is not measured, so the peak which developed in theory at that level is not detected. This value is estimated from the tangents of the measured bending moment distributions. The total amount of the anchor force has been measured, which is equivalent to the difference of the shear forces just above and below the anchor level. But the values of the shear forces are not known and therefore are estimated.

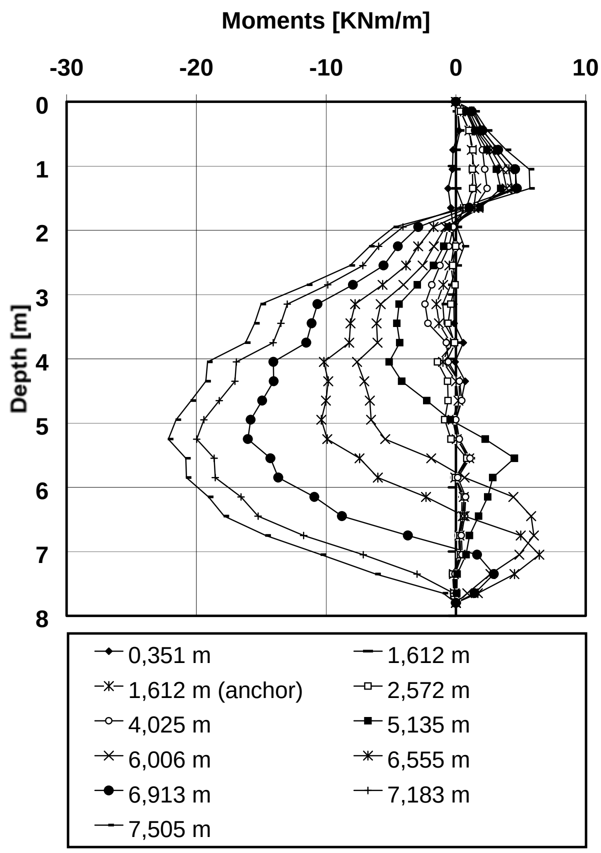

Figure 3 Bending moment distributions measured at different excavation depths

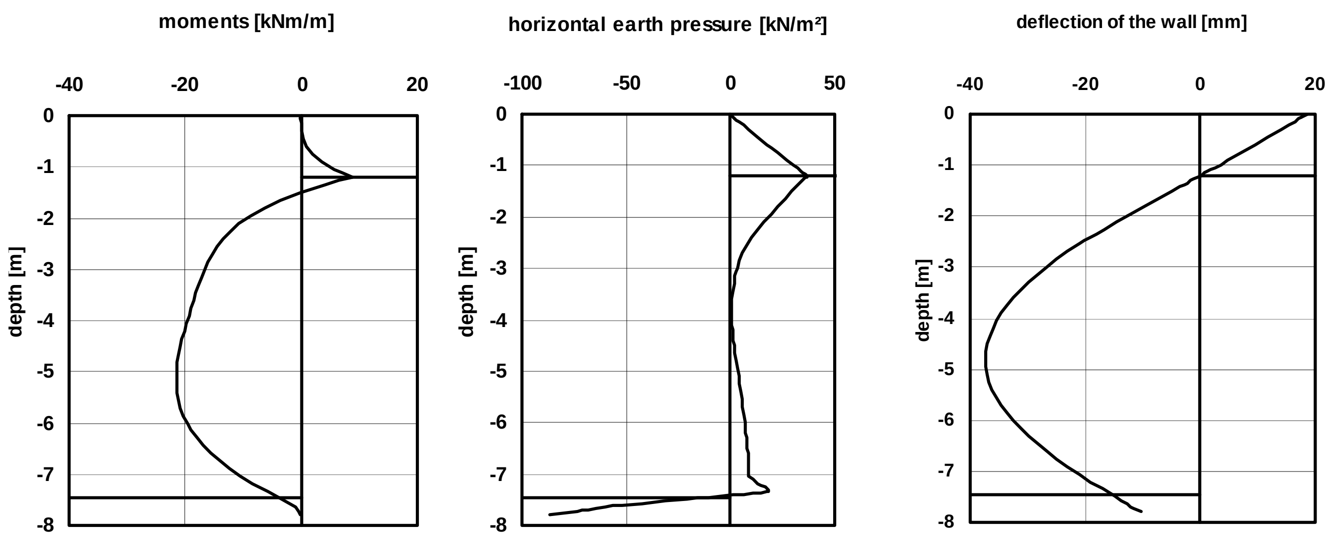

Figure 4 Fitted bending moments, earth pressure distribution, deflection of the wall examined for a test with density ρ = 1,69 g/cm³, anchor force A = 56,7 kN/m, wall stiffness EI = 3100 kNm²/m

Other tests have been performed to investigate the effect of wall plasticity on the response of varying wall system geometries (Bourne-Webb at al. 2011). In that case the excavation technique has been used successfully, but another challenge arose. In reality before formation of a plastic hinge within the sheet pile almost the full elastic wall bending stiffness would be available. The wall model was made from an aluminium plate with a weak section in the depth, where the plastic hinge formation has been expected. Due to this, large deformations corresponding to a strong bend of the wall within the weak section occurred with increasing excavation depth. These deformations caused extreme earth pressure reductions due to arching effects. This effect differs from the behaviour of a real sheet pile profile where elastic behaviour of the wall with constant stiffness dominates the deformation of the wall at the beginning of the excavation. At high excavation depth the formation of the plastic hinge would lead to a reduction of stiffness and a sudden increase of wall deformation. To reproduce this behaviour a more detailed wall model has to be developed showing a moment – curvature characteristic according to that of a real sheet pile profile.

3. TUNNELING

3.1 Methods

During the 1970`s and the 1980`s a model technique has been developed at the University of Cambridge (Potts 1976, Mair et al. 1984) in which air pressure is applied to control support conditions. This technique has been used later by e.g. Chambon et al. (1991) and König et al. (1991). The soil mass, which has to be removed during the excavation, is represented by a rubber membrane pressurized with air pressure. The shape of the rubber membrane is identical with the contour of the excavation. The equilibrium is kept between internal air pressure and external earth pressure during model preparation and increasing g-level. Initial stress conditions can be observed in the model after reaching the selected g-level. The excavation is simulated by decreasing the internal air pressure.

To keep equilibrium between internal air pressure and the earth pressure it would be necessary to apply internal support according to the theoretical earth pressure at state of rest. This support can not be achieved by the air pressure technique, because the air pressure remains constant along the contour of the excavation whereas the earth pressure varies with the change of orientation from vertical to horizontal and due to increase of vertical stress level with depth.

To overcome this problem Sharma et al. (2001) used a support by a rigid Styrofoam block instead of air pressure. The Styrofoam block covered by a rubber bag is dissolved by a solvent injected by pipes to reduce the support of the excavation zone. Yeo et al. 2010 discussed these two methods. Corresponding to the simulation technique for construction pits developed by Bolton et al (1988) they used a Zinc chloride solution for stabilizing the excavation zone before modelling the excavation process by releasing the fluid pressure. These techniques are mainly used for analysing failure mechanisms and limit state conditions.

Other techniques have been presented to study single processes during tunnelling by Bezuijen & van der Schrier (1994) and Yoshimura et al. (1994). Bezuijen & van der Schrier (1994) focused on the interaction between shield tunnelling process and an existing pile foundation. The influence of the gap between tunnel lining and soil behind the shield tail on the displacement field in the soil and the pile foundation was modelled by using a two dimensional tunnel model of which the diameter can be reduced. In this case only the part of the process was modelled which seems to be most important for the investigated phenomenon. The complete tunnelling process was not modelled,. Another solution for this task has been demonstrated by Farrell & Mair (2010). They modelled the volume loss taken place during a tunnelling process in a two dimensional model (plain strain conditions) by withdrawing a fluid out of an fluid filled annulus between the model tunnel lining and outer latex rubber lining.

Yoshimura et al. (1994) have investigated the influence of a shield tunnelling process on an existing tunnel. The existing tunnel is located parallel to a tunnel which is under construction. The effect of the shield tunnelling process on the stress strain conditions in the soil and the existing tunnel have been simulated by applying support pressure of varying magnitude on the face plate of a model shield. In this case an excavation process was not modelled. To study the failure mechanism in front of a collapsing tunnel face and to determine the minimum support pressure for stabilizing a tunnel face different authors used a rigid support of the tunnel face. This support is moved backwards to simulate the decrease of support pressure (Walter et al. 2010) or forward to activate passive earth pressure conditions (Wong et al.2010). In all these cases an in-flight excavation process was not realised.

In 1994 Nomoto et al. presented a miniature shield machine, which allowed the in-flight excavation of soil and also the in-flight installation of the lining. The soil is scraped by a cutting well and transported by a screw conveyor to the outside. The cutting head is pushed forward into the soil followed by a tube, which diameter is slightly smaller than the one of the cutter. This tube simulates the lining.

3.2 Bochum in-flight excavator for tunnelling

3.2.1 Design

The Bochum in-flight excavator (König 1998) is designed for modelling one step of a tunnel excavation in a silty sand with low water content and to analyze stress redistributions around the excavation area at the tunnel face initiated by the excavation process. An overview of the model with the in-flight excavator is given in Figure 5. The entire model is placed on a bottom plate. A strong box is housing the soil mass and supporting a hydraulic pressure jack as well as a carriage. The carriage can be moved horizontally by the hydraulic jack about ± 4 cm. This is equivalent to a maximum driving displacement of the in-flight excavator of 8 cm at model scale.

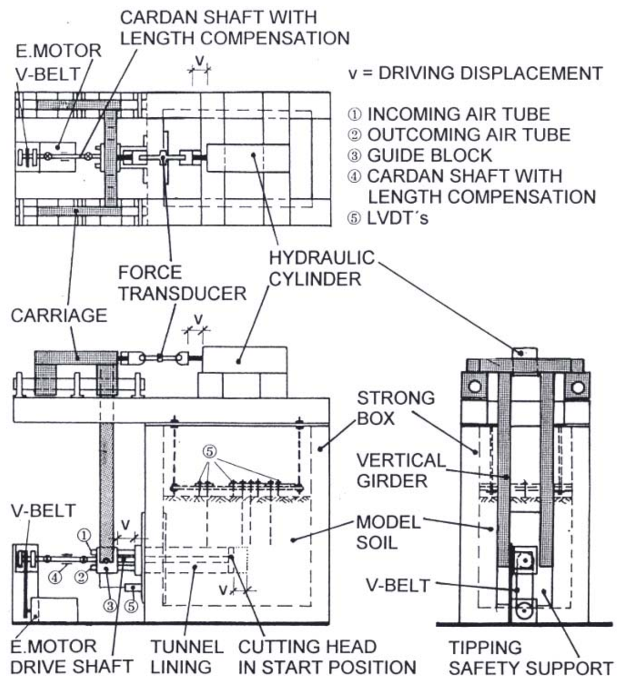

Figure 5 Setup of the model with in-flight excavator a) top view, b) side view, c) front view

The tunnel lining is placed inside the soil. The lining is supported in the front wall of the strong box. This support allows a vertical displacement, but impedes a tipping of the lining. The in-flight excavator is located inside of the tunnel lining. The cutting head is placed in start position inside the end of the lining in front of the tunnel face. The drive shaft of the excavator is connected by a cardan shaft with an electric motor. The cardan shaft allows a length compensation when the excavator is moved. The carriage is connected with the in-flight excavator by vertical girders and a guide block.

The in-flight excavator is presented in Figure 6 in detail. The excavator is supported in the tipping safety support. The excavator consists of the drive shaft with the cutting head and of six tubes. The six tubes and the drive shaft can be moved in longitudinal direction. The cut soil is transported to the outside of the strong box through three of the tubes by suction. The other three tubes allow air to flow behind the tunnel face and the cutting head to create an air flow in order to grasp all particles.

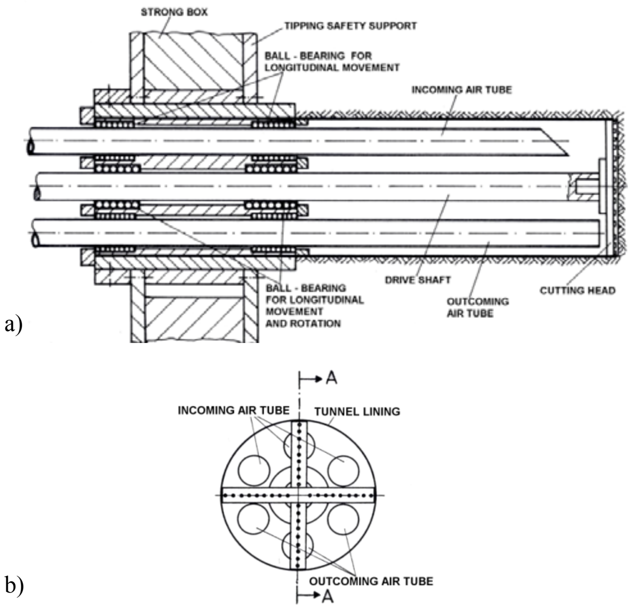

Figure 6 In-flight excavator a) section A-A, b) front view

During the excavation process surface settlement (Figure 5) are measured as well as vertical displacements close to the excavation by LVDT. Additional LVDT embedded in the soil are monitoring the horizontal displacements close to the excavation in the depth of the springline of the tunnel. Tangential strains of the tunnel lining are detected in crown, springline and invert at different distance from the end of the tunnel lining (4 measurement sections in 2.5, 10, 20 and 40 mm distance) by strain gauges. At least the force is measured by a force transducer necessary to move the cutting head forward.

3.2.2 Test procedure

The tipping safety support is installed in the strong box. The hole in tipping safety support system is closed. Now the strong box is filled with the model soil up to a given height. In this case it is either a mixture of fine sand (90 %), fine quartz (5%) and kaolin (5 %) with a water content of 2 % (model soil 2) or a mixture of fine sand (95 %), fine quartz (2.5%) and kaolin (2.5 %) with a water content of 1 % (model soil 3). The model soil is compacted to a given density. The strong box is placed in the swinging basket of the centrifuge and accelerated up to the selected g-level. After consolidation the machine is stopped and the model is removed from the basket.

Now the hole in the tipping safety support is opened and by the use of the in-flight excavator a cylindrical cavity is excavated which diameter is slightly less than the outer diameter of the tunnel lining. The tunnel lining is inserted into this cavity and fixed in the tipping safety support. The soil cut during the placement of the lining is sucked out. Now the in-flight excavator is placed inside the lining. The cutting head is located inside the end of the lining directly in front of the tunnel face.

After installation of all the equipment described above and also of the measurement devices the complete model is placed in the swinging basked of the centrifuge and is accelerated to the selected g-level. Initial stress conditions can be observed after a short reconsolidation time. Then the excavation starts.

The cutting head is rotated by the electric motor. At same time the cutting head is pushed forward into the soil by the hydraulic cylinder. The force of the cylinder is transferred by the carriage and the vertical girders to the guide block and from there to the drive shaft and the cutting head. The hydraulic cylinder is operated with constant displacement rate. The released soil is sucked out through the three lower tubes.

3.2.3 Test results

From the readings of the strain gauges the change in normal force in the tunnel lining due to one excavation step is calculated. The changes of normal forces determined in one measurement section at one distance from the end of the lining were nearly the same in crown, springline and invert and so the average value has been calculated. This change in normal force in the tunnel lining ΔN has been normalized by the unit weight of the soil γ and the square of the diameter of the tunnel D and plotted versus the normalized distance from the end of the lining a/D in Figure 7.

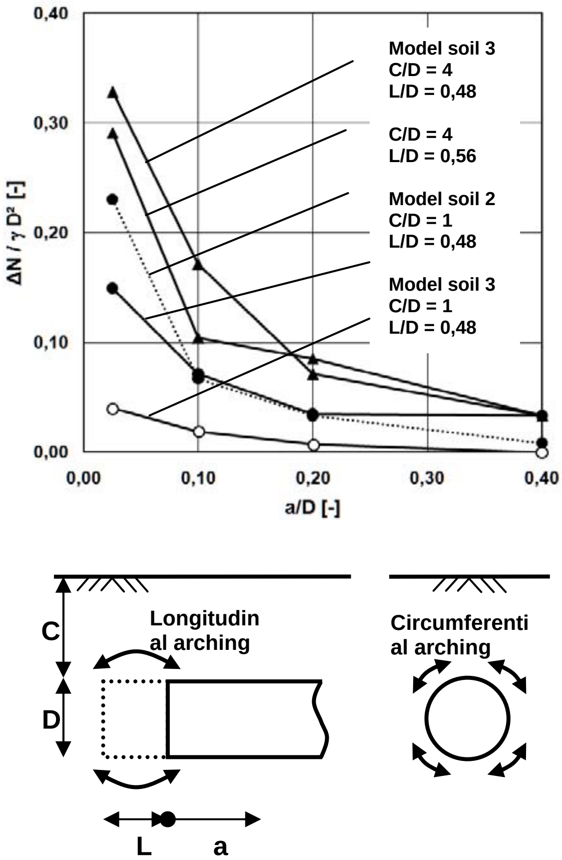

Figure 7 Normalised change in lining normal force $\Delta N/\gamma D^2$ due to one excavation step versus normalized distance from the end of the lining a/D (γ unit weight of soil, D diameter of tunnel, C soil cover from tunnel crest, a distance from end of tunnel lining, L excavation length)

Increased normal forces are detected at the end of the lining. This increase may be caused by a longitudinal arching, which is mobilised due to movements into the excavation and which loads the stable soil in front of the tunnel face and the tunnel lining. This longitudinal arch is acting simultaneous to a circumference arching effect.

The intensity of the longitudinal arching effect is increasing with excavation length L/D, with increase of cover in the range of a shallow tunnel (C/D = 1) and a deep tunnel (L/D = 4) and with decreasing soil stiffness (model soil 3 is stiffer then model soil 2) for the tested boundary conditions.

Figures 8 shows the excavation area for two tests after the tests have been finished and the models have been removed from the swinging basket and the soil mass have been cut. In the test with model soil 2 and a cover of C/D = 1 the excavation was not stable and collapse occurred. The shape of the failure mechanism is similar to the mechanism observed in other studies, but did not reach the surface although the cover was low. This and the squat form of the mechanism compared to similar mechanisms observed in sand (Chambon et al. 1991) is caused by the higher shear strength of the cohesive soil. In case of model soil 3 and C/D = 4 the excavated area was stable.

a)

b)

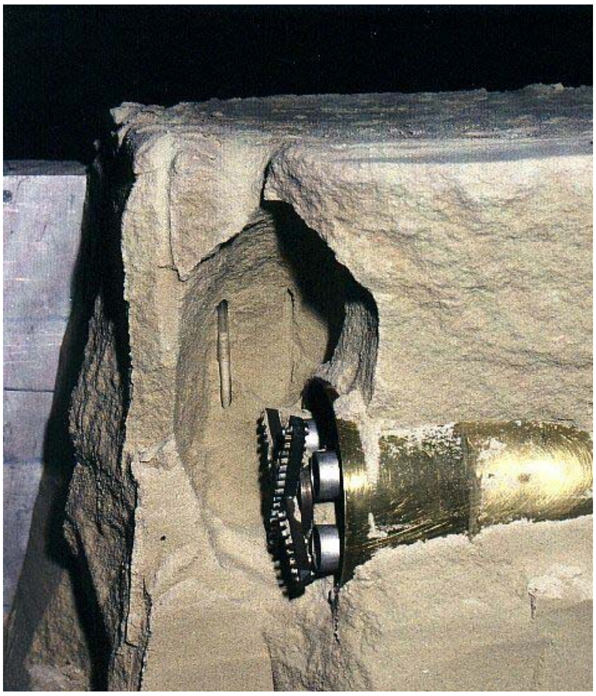

Figure 8 View of the unsupported cavity (excavation area) after the test a) in model soil 2 with a cover of C/D = 1 (collapse) and b) in model soil 3 with a cover of C/D = 4 (stable)

4. DEPOSITS

4.1 Methods

To simulate the construction of an embankment in a geotechnical centrifuge under increased gravity two methods are applied in general, fixed and movable hoppers. Davies & Parry (1985) described a hopper consisting of a number of cells with an outlet at the bottom which can be opened or closed by a two-way solenoid valve system. The hopper is installed on top of the strong box and each cell is filled with sand before the model is accelerated to the selected g-level. For constructing the embankment in-flight, the cells are opened and a layer of the embankment is poured. The geometry and thickness of the layer depend on the position of the cells, the amount of sand within each cell and on the opening time. By filling only a part of the cells of the hopper the geometry of the embankment can be adapted. For defining which cells should be filled to reach a certain geometry of the embankment the Coriolis effect has to be taken into account. This effect occurs when particles, are released from a part of the rotating model, e.g. from a hopper. These particles move independent from the rotating system and follow their own trajectories, which are different from the movement of the model (Taylor 1995). The effect and its consequences can be predicted. Other hopper systems based on this concept have been developed, e.g. by Allard et al. (1994).

4.2 Adaptive foundation system for an embankment on soft soil

Allersma (1994) gave details on a hopper system working with a movable funnel. Before accelerating the centrifuge the funnel is filled with sand. At increased g-level the outlet is opened and sand starts to sprinkle on the model surface. Simultaneously the hopper is moved. The geometry of the embankment depends on the amount of sand flowing out of the funnel and on the speed of the hopper. Also in this case the Coriolis effect has to be taken into account for predicting the final geometry of the embankment. The device used for the investigations performed in Bochum follows the principle of a moving hopper system.

The placement of embankments on very soft soil requires foundation works. Within a research project a new innovative adaptive foundation system for such situations is analysed by means of numerical calculations and centrifuge model tests in cooperation between HUESKER Synthetic GmbH and Ruhr-Universität Bochum.

The adaptive foundation (Figure 9) system consists of two vertical and parallel walls (e.g. sheet pile walls) which are introduced at a certain distance between each other into the soft soil and connected to each other by a tension membrane (e.g. geotextile) at the existing ground level. The vertical walls may end within the soft soil layer or reach further down into a firm layer. The soft soil beneath the embankment is therefore confined by the vertical and horizontal elements. The embankment is constructed above the tension membrane. The load from the embankment onto the soft soil generates a horizontal pressure onto the vertical walls which provokes outward movements. These movements are restricted by the tension membrane. At the same time an additional tension force is mobilized within the membrane due to settlements beneath the embankment. This additional tension force may lead to a further restriction of the outward movements. The foundation system ensures the global stability of the embankment (e.g. bearing failure and extrusion) and prevents or reduces the system deformations.

The stress and strain of the different system components, vertical walls, tension membrane and soft soil, are strongly influenced by their interaction. Due to consolidation processes in the soft soil these interactions are time dependent. So the stiffness of the soil as well as the total stress on the walls are changing with the consolidation from undrained condition at the beginning of the embankment construction to drained conditions in the final state. The system behaviour strongly depends on the distance between the vertical walls, their length and degree of fixation. Furthermore it depends on the thickness, shear strength and stiffness of the soft soil layer as well as the bending stiffness of the vertical walls and tension stiffness of the membrane and the relation of the latter both between each other. Within a series of centrifuge model tests some principle configurations of the systems should be analysed before starting a systematic investigation by numerical simulations. In the centrifuge model tests only the half of the system is modelled to take advantage of its symmetry. Therefore a hopper system has been developed to build up a half embankment under increased acceleration in three layers. This system will be described.

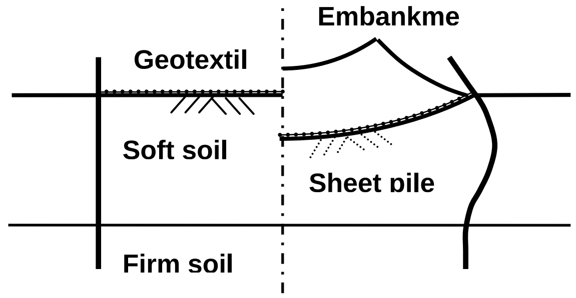

Figure 9 Adaptive foundation system for an embankment on soft soil, a) undeformed system before placing of the embankment, b) deformed system some time after placing the embankment

4.3 Bochum hopper system and test set up

4.3.1 Design of the hopper system

The hopper (Figure 10) was developed to allow the staged construction of the embankment in-flight and is mounted on top of the strong box. The device consists of a funnel (1) with a variable opening slit and a storage drum (2). The funnel is driven by a threaded rod (3) which is attached to a motor (4) and can move horizontally forwards and backwards along two steel bars (5). The speed of the funnel is fully adjustable. The sand can flow out from the funnel through a slit which opening width was calibrated in preliminary tests to allow for a well defined and regular sand flow. In start position as shown in Figure 10 this slit is blocked.

Once the funnel is empty it can be refilled in-flight from a storage drum (2). Therefore the storage drum can be rotated by an electric motor (6) and a gear system (7). The sand volume which is poured into the funnel through a 5 cm wide opening slit can be controlled by the rotation angle of the drum.

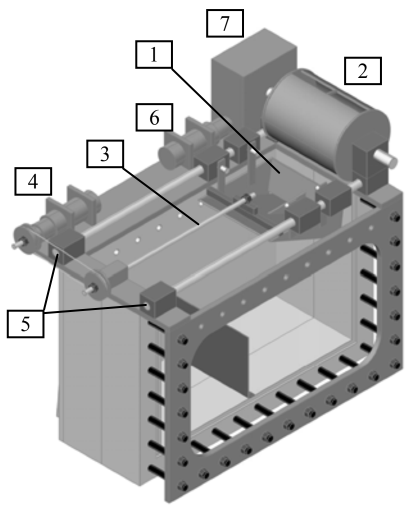

Figure 10 Bochum hopper system mounted on the strong box. Explanations see text

4.3.2 Test set up

A detailed description of the test set up is given by Detert et al. (2012). Two similar strong boxes are used for the test series. The inner dimensions of the strong boxes are 90 cm width, 36 cm depth and 60 cm height. One side wall is made out of acrylic glass to observe the system during the test. The thickness of the soft soil layer and the height of the embankment are 20 cm. The embankment width is 40 cm and the crest width about 5 cm. The soft soil layer is consolidated out of a Kaolin slurry. A 20 mm sand drainage layer is placed beneath the slurry. A geotextile is located in between the sand and the slurry as a separation and filtration layer. As only half of the system is modelled only one sheet pile wall model made of an aluminium plate is used. In the axis of symmetry at the side wall of the strong box the horizontal displacement of the geotextile should be zero whereas vertical movements should be allowed. This is realised by a special bearing element. The geotextile is fixed on one side to the model wall and at the other side to this special bearing element. Down-scaled geogrids according to Springman et al. (1992) are used for modelling the tension membrane.

4.3.3 Instrumentation

During the centrifuge tests total vertical pressure and pore water pressures are measured at various positions. The aluminium wall is instrumented with strain gauges at the centre line. At the connection between aluminium wall and geogrid two load cells are installed to measure the connection forces. Two displacement transducers are fixed to the top end of the aluminium wall to measure the horizontal displacements. A draw-wire sensor is attached to the geogrid bearing device at the axis of symmetry to detect vertical displacements. Two more displacement transducers measure the settlement of the Kaolin surface during the entire test.

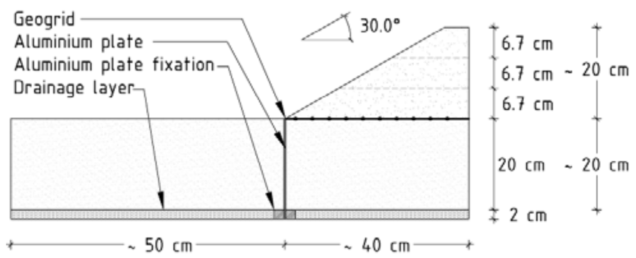

Figure 11 Centrifuge test set-up geometry

4.3.4 Test procedure

First the model wall is placed in the strong box in its final position and also the bearing element with the geotextile is installed, but the geotextile is not connected to the model wall at this time. A slurry prepared from Kaolin and water (w = 100 %) is filled in the strong box and is consolidated in the centrifuge at 50 g preparing a normally consolidated soft soil (OCR ~ 1). Since the consolidation takes a long time, two strong boxes are prepared and consolidated simultaneously in the two baskets of the beam centrifuge. After consolidation of the slurries, the centrifuge is stopped and one strong box is replaced by counterweights for the next test phase.

Excess Kaolin is extracted from the surface of the clay layer so the total height of the soft soil layer becomes 20 cm. The geogrid including the load cells is now connected to the aluminium plate and the hopper mechanism is mounted. After spinning up the model to 50 g and a reconsolidation phase of about 1 to 2 hour the embankment is constructed in three stages. In each stage a layer thickness of 1/3 of the final height is poured. A consolidation phase follows after each construction step.

4.4 Test results

Figure 12 shows the sequence of embankment construction at an acceleration level of 50 g. The toe of the embankment is in direct contact with the upper edge of the model wall, which exceeds the surface of the soft clay. Besides the model wall the clay is slightly coloured close to the contact surface with the Perspex glas. This is for getting a better contrast for evaluating the displacement field around the wall by digital image correlation technique from additional camera sequences. The lighting of the front side of the strong box is optimized for the additional digital cameras observing the soil mass beside the model walls.

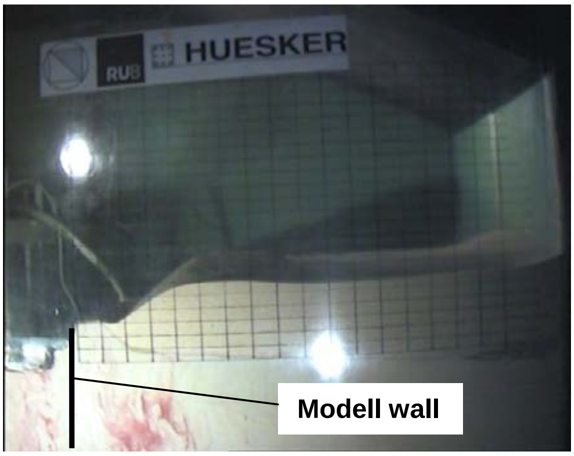

a)

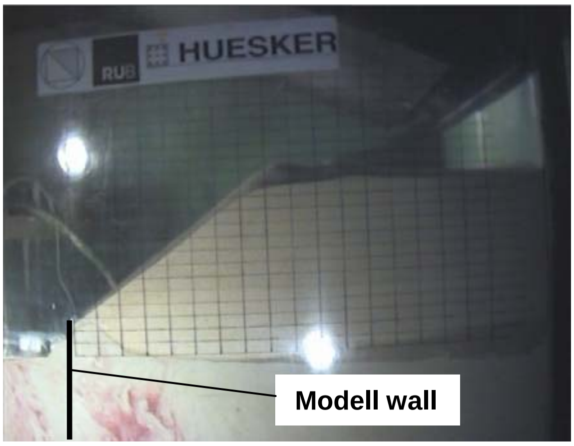

b)

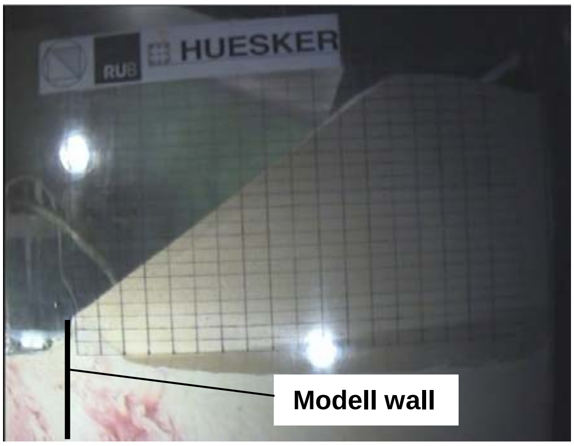

c)

Figure 12 Construction of the embankment under increase acceleration in three stages

A slightly deformed clay surface is visible at the first construction step (Figure 12 a). With increasing time and increasing height of the embankment (Figures 12 b and c) settlements of the clay surface are observed, which show a maximum in the middle of the system (axis of symmetry, side wall of strong box). Compared to a conventional basal reinforced embankment, where significant settlements can be also observed under the toe of the embankment, in this case the settlement contour vanish towards the model wall and a heave of the clay close to the wall is obvious. The subsoil is displaced by the embankment weight towards the side but captured by the vertical wall and horizontal tension membrane. The soft soil extrusion process is prevented by the foundation system. This shows the influence of the combined system of the walls connected with the tension membrane on the deformation behaviour.

The readings of the total stress transducer 7, located beside of the embankment, and of total stress transducer 3, located below the embankment, at the bottom of the clay layer are presented in Figure 13. The measured total stress is plotted versus time. The origin of the time axis corresponds to the start of the centrifuge. First the reconsolidation of the clay has taken place before the embankment is constructed in the three stages. In addition the total stress values are marked, which have been predicted analytically from layer thickness, soil density and acceleration.

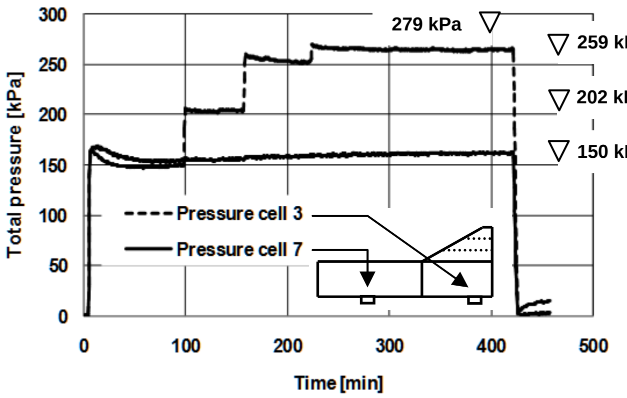

Figure 13 Readings of total pressure cells during reconsolidation and embankment construction versus time (model dimensions) and predicted total stress values for each construction stage (triangles)

Pressure cell 7 outside of the embankment detects constant total stress close to the predicted value. Pressure cell 3 below the embankment shows at the beginning similar total stress to cell 7. With construction of the embankment total stress is increasing. After the first construction step the measured total stress matches well the predicted value. With further construction steps an increasing discrepancy between measured and predicted total stress is observed. This may be caused by the contribution of the tension membrane to the load transfer of the self weight of the embankment. The tension membrane transfers a part of the load to the vertical structure elements.

The bending moment distribution of the model wall measured before and right after construction of second embankment layer as well as after 1 h consolidation is shown in Figure 14. The distribution is typical for a wall embedded at the toe and supported at the top. Due to the construction of the new layer of the embankment the bending moments increase. With ongoing consolidation the bending moments decreases significantly. This decrease corresponds to excess pore pressure dissipation, increase of effective stress and therefore reduction of earth pressure coefficient. The vertical structure elements in combination with the tension membrane restrict the horizontal deformation of the soil block below the embankment and lead to a stress concentration with corresponding consolidation process. Due to this the soil below the embankment gains shear strength and stiffness.

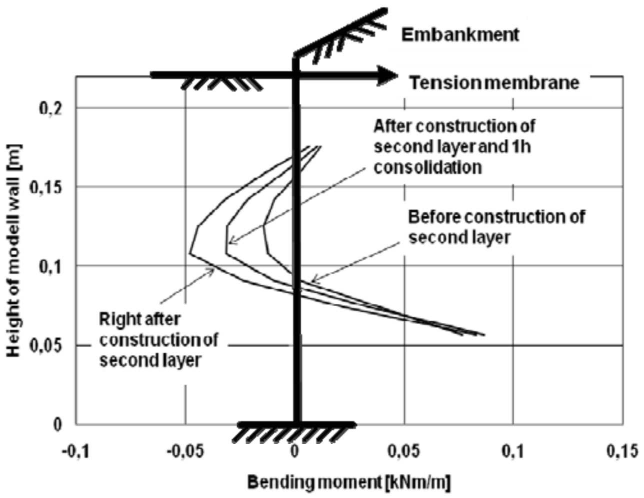

Figure 14 Bending moments distribution of the model wall before and right after construction of second embankment layer as well as after 1 h consolidation (model dimensions)

5. CONCLUSION

An overview is given on concepts and techniques to realize soil movements in centrifuge model testing under increased gravity related to the simulation of deep excavations, tunnelling and embankment construction. It is shown that also under increased acceleration complex excavation or deposit procedures can be simulated. Modern control and measurement systems will broaden the technical capabilities and will expedite the developments.

The various methods show different levels of complexibility to display the real processes more or less detailed. To support an excavation area by a fluid or air pressure at 1g acceleration and during spinning up the centrifuge until the selected acceleration level is reached and to model the excavation by the release of the pressure is an approved method and can be conducted with relatively low technical effort. A corresponding test design can be developed and prepared within a short time. On the other side this leads to different stress paths in the soil compared to the real situation. The differences in stress path can be reduced by increasing the degree of detailing of the excavation equipment. The development of such systems is more costly and time consuming. Robot systems acting in 2D or 3D space allow a manifold adaption and more economic test designs although complex construction procedures are simulated.

The choice on an adequate technique depends on the aim of the tests. Whereas failure mechanisms could be sufficiently triggered and visualized with simplified techniques to capture changes in stress and strain for small deformations e.g. in the state of serviceability the modelling of correct stress paths requires more complex techniques. But in all cases it is important to figure out the processes dominating the mechanisms and effects which want to be discovered for the field situation. These processes should be modelled carefully under idealized but well defined boundary conditions.

6. REFERENCES

Allard, M.A., Hjortnaers-Pedersen, A.G.I., Out, J.G. (1994) “Performance of a sand hopper”, Proc. of Int. Conf. Centrifuge 94, Singapore, Balkema, pp. 83-88

Allersma, H.G.B. (1998) “Development of cheap equipment for small centrifuges”, Proc. of Int. Conf. Centrifuge 98, Tokyo, Balkema, pp. 61-67

Allersma, H.G.B. (1994) “The university of delft geotechnical centrifuge”, Proc. of Int. Conf. Centrifuge 94, Singapore, Balkema, pp. 47-52

Azevedo, R. (1983) “Centrifugal and analytical modelling of excavations in sand”, Phd University of Colorado

Azevedo, R.F. (1988) “In-flight centrifuge excavation tests in sand”, Proc. of Int. Conf. Centrifuge 88, Paris, Balkema, pp. 119-124.

Bezuijen, A, Schrier, J van der (1994) “The influence of a bored tunnel on pile foundations” Proc. of Int. Conf. Centrifuge 94, Singapore, Balkema, pp. 681-692

Bourne-Webb, P.J., Potts, D., König, D., Rowbottom, D. (2011) “Analysis of model sheet pile walls with plastic hinges”, Geotechnique, 61/6, pp. 487 –499

Bolton, M.D., Powerie, W., Stewart, D.I. (1988) “The design of deep in-situ walls”, Proc. of Int. Conf. Centrifuge 88, Paris, Balkema, pp. 405-414

Chambon, P., Corté, J.F., Garnier, J., König, D. (1991) “Face stability of shallow tunnels in granular soils” Proc. of Int. Conf. Centrifuge 94, Boulder, Colorado, Balkema, pp. 99 – 106

Davies, M.C.R., Parry, R.H.G. (1985): “Centrifuge modeling of embankments on clay foundations”, Soils and Foundations, Vol. 25, No. 4, pp. 19-36

Derkx, F., Merliot, E., Garnier, J., Cottineau, L.M. (1998) “On board remote-controlled centrifuge robot”, Proc. of Int. Conf. Centrifuge 98, Tokyo, Balkema, pp. 97-103

Detert, O., König, D., Schanz, T. (2012) “Centrifuge modeling of an adaptive foundation system for embankments on soft soils”, Geotechniek, 10/2012, pp. 46-49

Furrel, R.P., Mair, R.J. (2010) “Centrifuge modeling of the response of buildings to tunneling” Proc. of ICPMG 2010, Zürich Switzerland, Balkema, pp. 549-554

Haigh, S.K., Houghton, N.E., Lam, S.Y., Li, Z., Wallbridge, P.J. (2010) “Development of a 2D servo-actuator for novel centrifuge modeling” Proc. of ICPMG 2010, Zürich Switzerland, Balkema, pp. 239-244

Gaudin, C., Garnier, J., Gaudicheau, Rault, G. (2002) “Use of a robot for inflight excavation in front of a embedded wall” Proc. of ICPMG 2010, St. John’s, Canada, Sweets & Zeitlinger Lisse, pp. 77-82

Jessberger, H.L., Güttler, U. (1988) “Bochum geotechnical centrifuge”, Proc. of Int. Conf. Centrifuge88, Paris, Balkema, pp. 37-44.

Kimura, T., Takemura, J., Hiro-oka, A., Okamura, M., Park, J. (1994) “Excavation on soft clay using in-flight excavator”, Proc. of Int. Conf. Centrifuge94, Singapore, Balkema, pp. 649-654

Kimura, T., Takemura, J., Hiro-oka, Suemasa, N., Kohda, M. (1993) “Stability of unsupported and supported vertical cuts in soft clay”, Proc. of 11th Southeast Asian Geotech. Conf., Balkema, pp 61-70

König, D. (2002) “Modeling of deep excavations”, Proc. of ICPMG 2010, St. John’s, Canada, Sweets & Zeitlinger Lisse, pp. 83-88

König, D. (1998) “An inflight excavator to model a tunneling process” Proc. of Int. Conf. Centrifuge 98, Tokyo, Balkema, pp. 707 – 712

König, D. Güttler, U., Jessberger, H.L. (1991) “Stress redistributions during tunnel and shaft constructions”, Proc. of Int. Conf. Centrifuge91, Boulder, Colorado, pp 129 – 135

Lade, P.V., Jessberger, H.L., Makowski, E., Jordan, P. (1981) “Modelling of deep shafts on centrifuge tests”, Proc. of 10th ICSMFE, Vol. 1, pp. 683-691

Lam, S.Y., Elshafie, M.Z.E.B., Haigh, S.K., Bolton, M.D. (2010) “Centrifuge modeling of deep excavation in soft clay”, Proc. of ICPMG 2010, Zürich Switzerland, Balkema, pp. 475-480

Loh, C.K., Tan, T.S., Lee, F.H. (1998) "Three-dimensional excavation tests", Proc. of Int. Conf. Centrifuge 98, Tokyo, Balkema, pp. 650 – 655

Lyndon, W., Pearson, R.A., (1984) "Pressure distribution on a rigid retaining wall in cohesionless material", Proc. of Symp. on the application of centrifuge modeling to geotechnical design, Manchester

Mair, R.J., Rain, P., Schofield, A.N., Taylor, R.N. (1984) "Application of centrifuge modeling to the design of tunnels and excavations in soft clay" Proc. of Int. Symp. "The application of centrifuge modeling to geotechnical design", Craig, W.H. (editor), Manchester, pp. 356-366

Nomoto, K., Mito, K., Imamura, S., Ueno, K., Kusakabe, O. (1994) "A miniature shield tunneling machine for a centrifuge", Proc. of Int. Conf. Centrifuge94, Singapore, Balkema, pp. 699-704

Potts, D.M. (1976) "Behavior of lined and unlined tunnel in sand" PhD Thesis, Cambridge University, Churchill College

Schürmann, A., Jessberger, H.L. (1994) "Earth pressure distribution on sheet pile walls", Proc. of Int. Conf. Centrifuge94, Singapore, Balkema, pp. 95-100

Springman, S., Bolton, M., Sharma, J., Balachandran, S. (1992) "Modelling and instrumentation of a geotextile in the geotechnical centrifuge. In H. Ochiai, S. Hayashi and J. Otani (Eds.) , Proc. of Int. Symp. On Earth Reinforcement Practice, Balkema, Rotterdam, pp. 167–172

Shama, J.S., Bolton, M.D., Boyle, R.E. (2001) "A new technique for simulation of tunnel excavation in a centrifuge", ASTM Geotechnical testing Journal, 24 (4), pp. 343-349

Taylor, R.N. (1995) "Geotechnical centrifuge technology" Chapmann & Hall, ISBN 0 7514 0032 7

Toyosawa, Y, Horii, N., Tamate, S., Hanayasu, S., Ampadu, S.K. (1994) "Deformation and failure characteristics of vertical cuts and excavations in clay", Proc. of Int. Conf. Centrifuge 94, Singapore, Balkema, pp. 655-663

Walter, H., Coccia, C.J., Wallen, R.B., Ko, H.Y., McCartney, J.S. (2010) "Modelling of a tunnel lining deformation due to face instability" Proc. of ICPMG 2010, Zürich Switzerland, Balkema, pp. 593-598

Wong, K.S., Ng, C.W.W., Chen, Y.M., Bian, X.C. (2010) "Centrifuge modeling of passive failure of tunnel face in saturated sand" Proc. of ICPMG 2010, Zürich Switzerland, Balkema, pp. 599-604

Yeo, C.H., Lee, F.H., Hegde, A., Juneja, A. (2010) "Centrifuge modeling of a steel pipe umbrella arch for tunneling in clay", Proc. of ICPMG 2010, Zürich Switzerland, Balkema, pp. 611-616

Yoshimura, H., Miyabe, K., Tohda, J. (1994) "Response of a tunnel lining due to an adjacent twin shield tunneling", Proc. of Int. Conf. Centrifuge 94, Singapore, Balkema, pp. 693-698

Zheng, G., Wei, S.W., Peng, S.Y., Diao, Y., Ng., C.W.W. (2010) "Centrifuge modeling of the influence of basement excavation on existing tunnels", Proc. of ICPMG 2010, Balkema, pp. 523-527